NIH Public Access
Author Manuscript
Conf Proc IEEE Eng Med Biol Soc. Author manuscript; available in PMC 2012 December 09.

Published in final edited form as:
Conf Proc IEEE Eng Med Biol Soc. 2011 ; 2011: 4665–4668. doi:10.1109/IEMBS.2011.6091155.

CaMKII-dependent Activation of Late I_{Na} Contributes to Cellular Arrhythmia in a Model of the Cardiac Myocyte

Yasmin L. Hashambhoy, **Raimond L. Winslow**, and **Joseph L. Greenstein**
Institute for Computational Medicine, Department of Biomedical Engineering, The Johns Hopkins University, Baltimore, MD 21218 USA.

Yasmin L. Hashambhoy: yhasham2@jhmi.edu; Raimond L. Winslow: rwinslow@jhu.edu

Abstract

Cardiac voltage-gated Na^+ channels underlie membrane depolarization during the upstroke of the action potential (AP). These channels also exhibit a late, slowly-inactivating component of current (late I_{Na}) that may be enhanced under pathological conditions such as heart failure, and may therefore promote AP prolongation and increase the likelihood of arrhythmia. Ca^{2+}/calmodulin-dependent protein kinase II (CaMKII) functionally modifies Na^+ channels, however it remains unclear if the CaMKII-dependent changes in late I_{Na} are a major contributor to cellular arrhythmias such as early after depolarizations (EADs). In this study we develop a model of I_{Na}, including CaMKII-dependent effects, based on experimental measurements. The Na^+ channel model is incorporated into a computational model of the whole myocyte which describes excitation-contraction coupling via stochastic simulation of individual Ca^{2+} release sites. Simulations suggest that relatively small augmentation of late I_{Na} is sufficient to significantly prolong APs and lead to the appearance of EADs.

I. Introduction

Cardiac voltage-gated Na^+ channels allow for the rapid influx of Na^+ into cardiac myocytes which drives membrane depolarization. These channels exhibit fast activation kinetics, and the inward Na^+ current (I_{Na}) is responsible for the rapid upstroke at the start of the cardiac action potential (AP). These Na^+ channels may also play an important role in setting the AP duration (APD). Mutations in the gene encoding the α-subunit of the Na^+ channel have been associated with long-QT syndrome as well as Brugada syndrome [1, 2]. Mutant channels exhibit slower recovery from inactivation as well as a negative shift in voltage-dependent availability. In addition, these channels exhibit "late I_{Na}", a relatively small persistent inward current that fails to fully inactivate during the AP and likely contributes to APD prolongation. Furthermore, studies have demonstrated that enhancement of late I_{Na} under conditions of oxidative stress, as may occur in heart failure, leads to AP prolongation and cellular arrhythmias such as early after depolarizations (EADs) [4].

Ca^{2+}/calmodulin –dependent protein kinase II (CaMKII) is a Ca^{2+}-dependent protein that regulates the function of a number of transporters, pumps, and ion channels via protein phosphorylation. CaMKII activity has been linked to alterations in Na^+ channel behavior and its expression has been shown to be increased in heart failure [5]. Recently, a number of notable studies have elucidated functional effects of CaMKII-mediated Na^+ channel phosphorylation. Deschenes et al [6] cloned Na^+ channels in HEK293 and C2C12 cells and

J. L. Greenstein (phone: 410-516-5425; fax: 410-516-5294; jgreenst@jhu.edu)

found that the CaMKII inhibitor KN-93 (but not the CaMKII inhibitor AIP) slowed current decay, shifted steady-state inactivation in the depolarizing direction, and slowed the kinetics of entry into inactivated channel states. Maltsev et al [7] found that in canine ventricular myocytes, late I_{Na} decay was accelerated by KN-93 in the presence of elevated cytosolic Ca^{2+} levels. Wagner et al [8] studied the effects of adenovirus mediated and transgenic CaMKII over-expression and observed that CaMKII over-expression caused a negative shift in the voltage dependence of Na^+ channel availability, enhanced intermediate inactivation, slowed recovery from inactivation, and increased the amplitude of late I_{Na}. The latter results form the basis for a CaMKII-dependent Na^+ channel computational model by Grandi et al [9].

While these previous experimental results revealed the functional importance of CaMKII-mediated phosphorylation of Na^+ channels, the acute effects of CaMKII on channel function remained unclear. Recently, Aiba et al [3] studied the direct effects of CaMKII on Na^+ channels in guinea pig ventricular myocytes. Using whole cell patch clamp techniques, they found that CaMKII-dependent phosphorylation caused a positive shift in the voltage dependence of Na^+ channel availability, hastened recovery from inactivation, and decreased intermediate inactivation. In addition, Aiba et al [3] also found that CaMKII-dependent phosphorylation increased late I_{Na}. These recent results are the basis for the Na^+ channel state model presented in this study, which describes the behavior of unphosphorylated and CaMKII-phosphorylated Na^+ channels based on a preexisting model [9]. It is further constrained by voltage- and temperature-specific I_{Na} kinetics, and it accounts for the acute effects of CaMKII phosphorylation on Na^+ channels. Furthermore, it has been integrated into our computational model of the canine ventricular myocyte [10] that describes excitation-contraction coupling via stochastic simulation of individual Ca^{2+} release sites (dyadic clefts) [11] with local CaMKII-mediated phosphorylation of L-type Ca^{2+} channels (LCCs) [12] and ryanodine receptors (RyRs) [10]. This allows us to use the model to isolate the role each CaMKII target plays in determining AP shape and duration.

II. Methods

The Na^+ channel model of Grandi et al [9] was used as a framework to build a model that could reproduce the recent experimental results of Aiba et al [3], who measured the acute effects of CaMKII on cardiac Na^+ currents in guinea pig ventricular myocytes in the presence of CaMKII or AIP. In order to constrain the model, it was assumed that in the presence of AIP all Na^+ channels were unphosphorylated, whereas upon the addition of CaMKII (without AIP), all channels were assumed to be phosphorylated. The experiments were performed at room temperature.

As in the model of Grandi et al [9], the Na^+ channel model presented here consists of two 13-state deterministic models; the first represents an unphosphorylated Na^+ channel and the second represents a CaMKII-phosphorylated channel. The transition rates within each of the models were re-fit to match the results of a variety of experimental protocols [3] including activation, steady-state availability, recovery from inactivation, intermediate inactivation and late I_{Na} amplitude, as described in [9]. Fig. 1 shows a comparison of model simulations and experimental data for I_{Na}.

Aiba et al [3] found that CaMKII phosphorylation of Na^+ channels increases late I_{Na} significantly. This discovery corroborates the findings of Wagner et al [8], who also found increased late I_{Na} in cardiac myocytes from transgenic mice over-expressing CaMKII and from myocytes in which CaMKII had been adenovirally over-expressed. When measured under voltage-clamp, late I_{Na} is $0.23 \pm 0.1\%$ of peak I_{Na} in both control and CaMKII inhibited myocytes, whereas it is $0.95 \pm 0.47\%$ of peak I_{Na} in cells that have been acutely

exposed to CaMKII [3]. After fitting model parameters, the model exhibits late I_{Na} with a magnitude of 0.16% of peak I_{Na} in unphosphorylated channels, and 0.79% of peak I_{Na} in phosphorylated channels. Experiments [3] showed that late I_{Na} is not significantly different between control and CaMKII-inhibited myocytes. Thus for the model, it was assumed that under control conditions Na^+ channels are unphosphorylated.

The transition rates within each model were scaled for body temperature. Studies have shown that Na^+ channel kinetics are considerably faster at 37°C (body temperature) than at 23°C (room temperature) [13]. In addition, Na^+ channel conductance has been shown to increase with temperature [14]. Nagatomo et al [13] found that the rate of I_{Na} decay increased ~3-fold from 23°C to 33°C. Rates were adjusted to match this temperature-dependent increase in kinetics at voltage clamp test potentials of −30 mV, −20 mV, −10 mV and 0 mV. All rates were increased by a factor of 2.5. Certain rates were further adjusted to match depolarizing shifts in activation curves at higher temperatures, as observed in experiments [14] and to maintain the sigmoidal shape of the activation and availability curves. Fig. 2 shows simulated I_{Na} at both room and body temperature for voltage clamps to −20 mV and 0 mV compared to I_{Na} data obtained at room temperature [3] for unphosphorylated and phosphorylated channels. I_{Na} decay rates increase by a factor of ~3–5 at body temperature. Transition rate definitions are identical to those described in [9], with the exception of a_6, which is now defined as $P_{1a4} \times e^{V/(P2a4 \times P2a4\_2)}/P_{1a6}$. Kinetic parameters of the Na^+ channel model are given in Table I.

It was necessary to fit the Na^+ channel model for channel conductance. Using the late I_{Na} magnitude reported by Valdivia et al [15], and accounting for reported temperature-induced increases in channel conductance [14], Na^+ channel conductance was fit and a value of 8 mS/μF was obtained.

Finally, minor adjustments to the whole cell model were made to fine tune AP properties in the presence of a new Na^+ channel model which now included significant late I_{Na}. The number of channels that carry the Ca^{2+}-dependent Cl^- current (I_{to2}) was set to the level originally reported by Greenstein and Winslow [11]. In addition, I_{K1} conductance was increased by 10%, in agreement with recent experimental measurements in canine myocytes [16].

III. Results

A. Rate Dependent AP Shape and Duration

Fig. 3A shows average simulated APs over 50 s (1Hz pacing) and 25 s (0.5 Hz and 2 Hz pacing). APD increases with cycle length, as in experimental data [16]. Average APD at 90% repolarization (APD_{90}) is 314.0 ± 7.2 ms during 2 Hz pacing, 383.3 ms ± 7.0 ms during 1 Hz pacing and 463.3 ± 23.8 ms during 0.5 Hz pacing (data are presented as mean ± S.E.M.). Experimental APD measurements are highly variable. The APD_{90} data presented by Li et al [16] in canine myocytes is close to that shown here (305 ms, 375 ms, and 422 ms at 2 Hz, 1 Hz, and 0.5 Hz pacing, respectively).

B. AP Duration and Late I_{Na}

Fig. 3B shows the relationship between fractional Na^+ channel phosphorylation and APD_{90}. As the fraction of Na^+ channels that are phosphorylated increases, so does APD. This result makes intuitive sense since late I_{Na} contributes significant inward current during the plateau of the AP. Profiles of average late I_{Na} at 0% and 10% Na^+ channel phosphorylation during 1 Hz APs are shown in Fig. 3C. Mean I_{Na} during the 100 ms to 300 ms time interval of the AP is −0.177 pA/pF and −0.265 pA/pF at 0% and 10% Na^+ channel phosphorylation, respectively. Due to late I_{Na} and significant increases in APD, occasional EADs are

observed in the simulated APs (see Fig. 3D). EAD frequency increases with fractional Na^+ channel phosphorylation.

C. Differential LCC and Na^+ Channel Phosphorylation

APD is very sensitive to both late I_{Na} and the late phase of the L-type Ca^{2+} current. In order to better understand APD variation with differential channel phosphorylation, simulations were performed in which the maximum CaMKII-mediated LCC phosphorylation rate and fractional Na^+ channel phosphorylation were varied (Fig. 4). The LCC phosphorylation model has been described previously [12].

When LCC phosphorylation rates remain at their control values (light grey curve) and there is no Na^+ channel phosphorylation, APD_{90} is 383 ms. APD_{90} increases steadily with increased fractional Na^+ channel phosphorylation, reaching 481 ms with 10% phosphorylated Na^+ channels. Under these conditions, EADs are observed at 4% Na^+ channel phosphorylation.

Decreasing LCC phosphorylation rates to 80% of normal (dark grey curve) lowers APD_{90} to 361 ms and 446 ms at 0% and 10% Na^+ channel phosphorylation, respectively. At this rate of LCC phosphorylation, EADs appear at 10% Na^+ channel phosphorylation. Lowering LCC phosphorylation rates to 60% of normal (black curve) diminishes APD_{90} to 350 ms and 416 ms at 0% and 10% Na^+ channel phosphorylation, respectively, and no EADs were observed.

IV. Discussion

The cardiac myocyte model presented here builds upon a Na^+ channel representation that accounts for more recently observed Na^+ channel gating phenomena, such as burst mode states. Simulations show that this model is able to reproduce features of I_{Na} at room temperature, and rate parameters have been scaled to match experimentally observed temperature-dependent shifts in gating properties.

With the addition of the new Na^+ channel model, the whole cell model contains two channels that conduct inward currents, carried by Na^+ and Ca^{2+}, which have augmented function as a result of CaMKII phosphorylation. Therefore, it is not surprising that APD is greatly augmented in comparison with results from our original model [11].

Our results indicate that APD and shape are highly sensitive to Na^+ channel phosphorylation. Even a small fraction of Na^+ channel phosphorylation has the potential to result in occasional EADs (see Fig. 3D). It should be noted that the experimental observations of late I_{Na} from Aiba et al [3] had a large amount of variability ($0.95 \pm 0.47\%$ of peak I_{Na} in phosphorylated channels). In simulations, the late I_{Na} produced by phosphorylated channels is 0.8% of peak. If the rate into the Na^+ channel burst mode states (see [9]), and thus late I_{Na}, were reduced, sensitivity to Na^+ channel phosphorylation would also decrease. Fig. 4 shows that the model is also very sensitive to LCC phosphorylation. Even a small reduction in CaMKII-dependent LCC phosphorylation rate, which leads to reduced occupancy of the LCC high activity gating mode (mode 2, see [12]), results in a significant decrease in APD.

This model is limited by the fact that it does not include dynamic CaMKII-mediated phosphorylation of Na^+ channels. We took the simple approach of assuming steady-state fractional phosphorylation of Na^+ channels because data on the dynamics of CaMKII-dependent Na^+ channel phosphorylation are not available, and therefore the associated rates cannot be reasonably constrained. Currently, the location of the Na^+ channel

phosphorylation site, as well as its phosphorylation and dephosphorylation rates, remains unknown. However, the model includes a representation of cytosolic CaMKII, so that when the phosphorylation rates become available, it will be relatively straightforward to describe dynamic transitions between unphosphorylated and phosphorylated Na^+ channels. Despite this model limitation, this study has helped further illustrate the sensitivity of the cardiac AP to Na^+ channel phosphorylation.

The model presented here has demonstrated a mechanistic link between augmentation of late I_{Na}, AP prolongation and the appearance of EADs in agreement with previous experimental observations [4]. Recently, the generation of reactive oxygen species under conditions of increased oxidative stress, such as during heart failure, has been linked to CaMKII-mediated enhancement of late I_{Na} and consequent arrhythmias [17]. Therefore, therapies that target late I_{Na}, such as block by ranolazine [18], may have promise in treating patients that are at risk for arrhythmia.

Acknowledgments

This work was supported in part by the National Institutes of Health under Grants R33HL87345 and PO1HL081427.

The authors thank Takeshi Aiba for providing I_{Na} data.

References

1. Bezzina C, et al. A Single Na+ Channel Mutation Causing Both Long-QT and Brugada Syndromes. Circ Res. 1999 Dec 3.vol. 85:1206–1213. 1999. [PubMed: 10590249]
2. Chen Q, et al. Genetic basis and molecular mechanism for idiopathic ventricular fibrillation. Nature. 1998; vol. 392:293–296. [PubMed: 9521325]
3. Aiba T, et al. Na+ channel regulation by Ca2+/calmodulin and Ca2+/calmodulin-dependent protein kinase II in guinea-pig ventricular myocytes. Cardiovasc Res. 2010 Feb 1.vol. 85:454–463. [PubMed: 19797425]
4. Xie L-H, Chen F, Karagueuzian HS, Weiss JN. Oxidative Stress-Induced After depolarizations and Calmodulin Kinase II Signaling. Circ Res. 2009 Jan 2.vol. 104:79–86. 2009. [PubMed: 19038865]
5. Kirchhefer U, Schmitz W, Scholz H, Neumann J. Activity of cAMP-dependent protein kinase and Ca2+/calmodulin-dependent protein kinase in failing and nonfailing human hearts. Cardiovasc Res. 1999 Apr.vol. 42:254–261. [PubMed: 10435018]
6. Deschenes I, et al. Isoform-Specific Modulation of Voltage-Gated Na+ Channels by Calmodulin. Circ Res. 2002 Mar 8.vol. 90:e49–e57. 2002. [PubMed: 11884381]
7. Maltsev VA, Reznikov V, Undrovinas NA, Sabbah HN, Undrovinas A. Modulation of late sodium current by Ca2+, calmodulin, and CaMKII in normal and failing dog cardiomyocytes: similarities and differences. Am J Physiol Heart Circ Physiol. 2008 Apr 1.vol. 294:H1597–H1608. 2008. [PubMed: 18203851]
8. Wagner S, et al. Ca²⁺/calmodulin-dependent protein kinase II regulates cardiac Na⁺channels. Journal of Clinical Investigation. 2006; vol. 116:3127–3138. [PubMed: 17124532]
9. Grandi E, et al. Simulation of Ca-Calmodulin-Dependent Protein Kinase II on Rabbit Ventricular Myocyte Ion Currents and Action Potentials. Biophys. J. 2007 Dec 1.vol. 93:3835–3847. 2007. [PubMed: 17704163]
10. Hashambhoy YL, Greenstein JL, Winslow RL. Role of CaMKII in RyR leak, EC coupling and action potential duration: a computational model. J Mol Cell Cardiol. 2010 Oct.vol. 49:617–624. [PubMed: 20655925]
11. Greenstein JL, Winslow RL. An integrative model of the cardiac ventricular myocyte incorporating local control of Ca2+ release. Biophys J. 2002 Dec.vol. 83:2918–2945. [PubMed: 12496068]

12. Hashambhoy YL, Winslow RL, Greenstein JL. CaMKII-induced shift in modal gating explains L-type Ca(2+) current facilitation: a modeling study. Biophys J. 2009 Mar 4.vol. 96:1770–1785. [PubMed: 19254537]
13. Nagatomo T, et al. Temperature dependence of early and late currents in human cardiac wild-type and long Q-T Delta KPQ Na+ channels. Am J Physiol Heart Circ Physiol. 1998 Dec 1.vol. 275:H2016–H2024. 1998.
14. Murray KT, Anno T, Bennett PB, Hondeghem LM. Voltage clamp of the cardiac sodium current at 37 degrees C in physiologic solutions. Biophys. J. 1990 Mar 1.vol. 57:607–613. 1990. [PubMed: 2155034]
15. Valdivia CR, et al. Increased late sodium current in myocytes from a canine heart failure model and from failing human heart. Journal of Molecular and Cellular Cardiology. 2005; vol. 38:475–483. [PubMed: 15733907]
16. Li G-R, Lau C-P, Ducharme A, Tardif J-C, Nattel S. Transmural action potential and ionic current remodeling in ventricles of failing canine hearts. Am J Physiol Heart Circ Physiol. 2002 Sep 1.vol. 283:H1031–H1041. 2002. [PubMed: 12181133]
17. Wagner S, et al. Reactive Oxygen Species-Activated Ca/Calmodulin Kinase II{delta} Is Required for Late INa Augmentation Leading to Cellular Na and Ca Overload. Circ Res. 2011 Mar 4.vol. 108:555–565. [PubMed: 21252154]
18. Rajamani S, El-Bizri N, Shryock JC, Makielski JC, Belardinelli L. Use-dependent block of cardiac late Na(+) current by ranolazine. Heart Rhythm. 2009 Nov.vol. 6:1625–1631. [PubMed: 19879541]

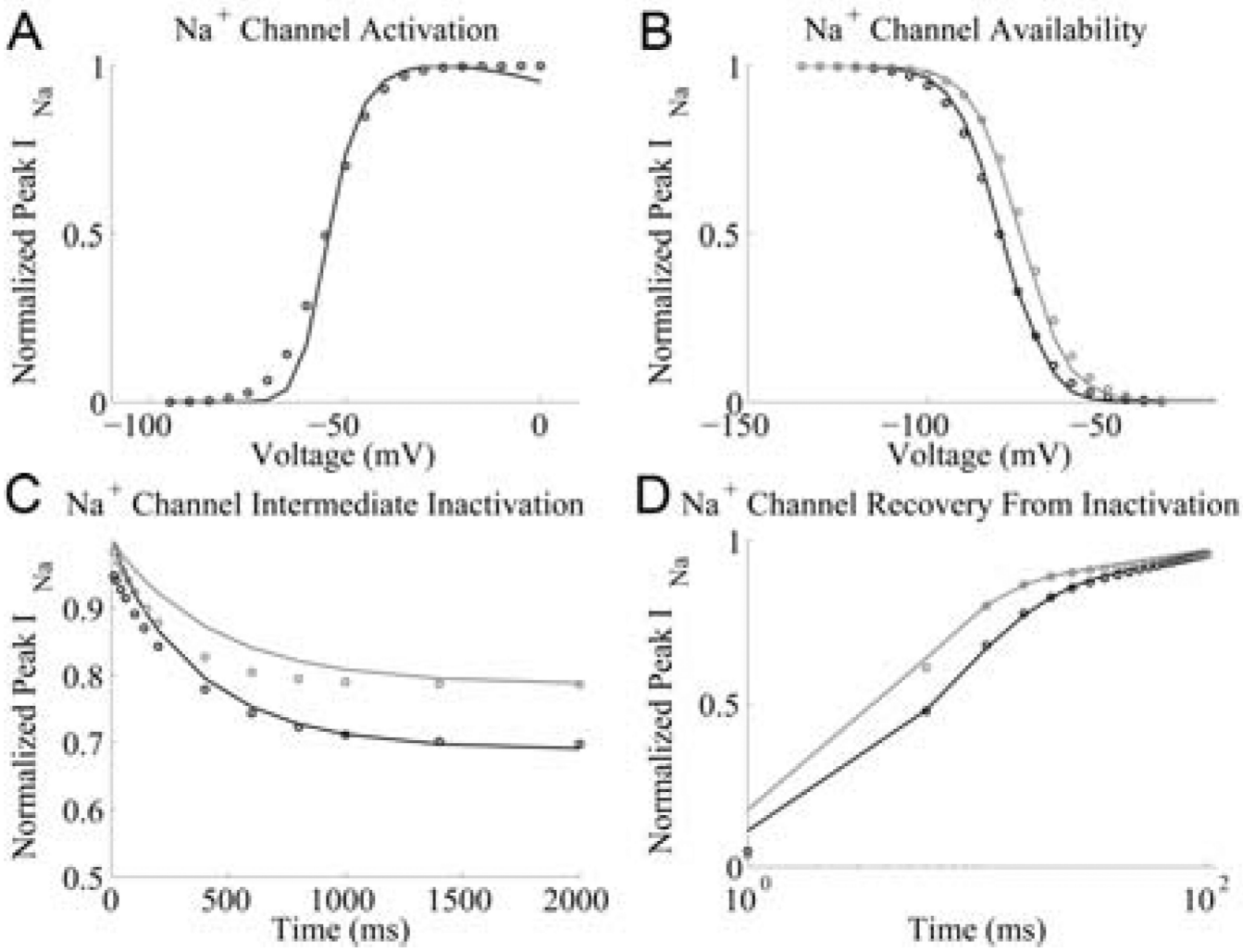

Fig. 1.

Na^+ channel model simulation (solid lines) and experimental data (circles) [3] under phosphorylated (grey) and unphosphorylated (black) conditions. (A) Activation: I_{Na} is recorded during a 50 ms test potential from a holding potential of −120 mV. (B) Availability: a 500ms prepulse to a variable voltage is followed by a voltage clamp to −20mV, during which I_{Na} is recorded. (C) Recovery from intermediate inactivation: holding potential of −140 mV is followed by a variable duration prepulse to −20mV, during which I_{Na} is recorded. The membrane is then clamped to −140 mV for 20 ms and then to −20 mV for 50 ms, during which I_{Na} is recorded again. The ratio of peak I_{Na} (−20 mV vs. prepulse) is shown as a function of prepulse duration. (D) Recovery from inactivation: a holding potential of −140 mV is followed by a prepulse to −20mV for 300 ms, during which I_{Na} is recorded. The membrane is then clamped to −140 mV for a variable duration and then clamped to −20 mV for 50 ms, during which I_{Na} is recorded again. The ratio of peak I_{Na} (2^{nd} vs. 1^{st} pulse) is shown as a function of the interpulse interval.

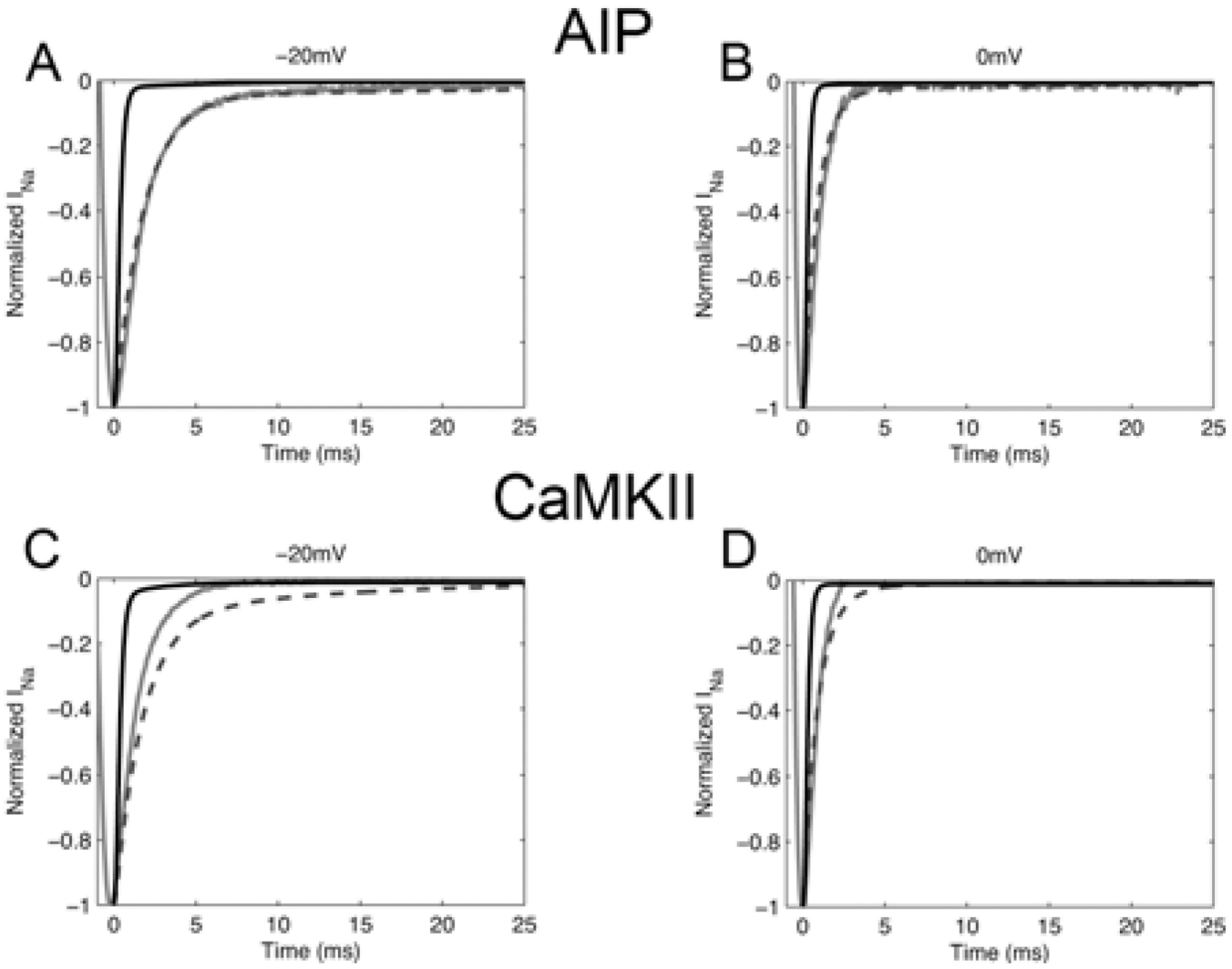

Fig. 2.

Simulated vs Experimental I_{Na} under voltage clamp. A 50 ms test clamp was applied from a holding potential of −120 mV. Experimental results [3] at 23°C in guinea pig myocytes (solid grey line) are compared with simulated I_{Na} at 23°C (dashed line) and 37°C (solid black line). I_{Na} is shown in the presence of CaMKII inhibitor AIP at −20 mV (A) and 0 mV (B) and in the presence of CaMKII at −20 mV (C) and 0 mV (D).

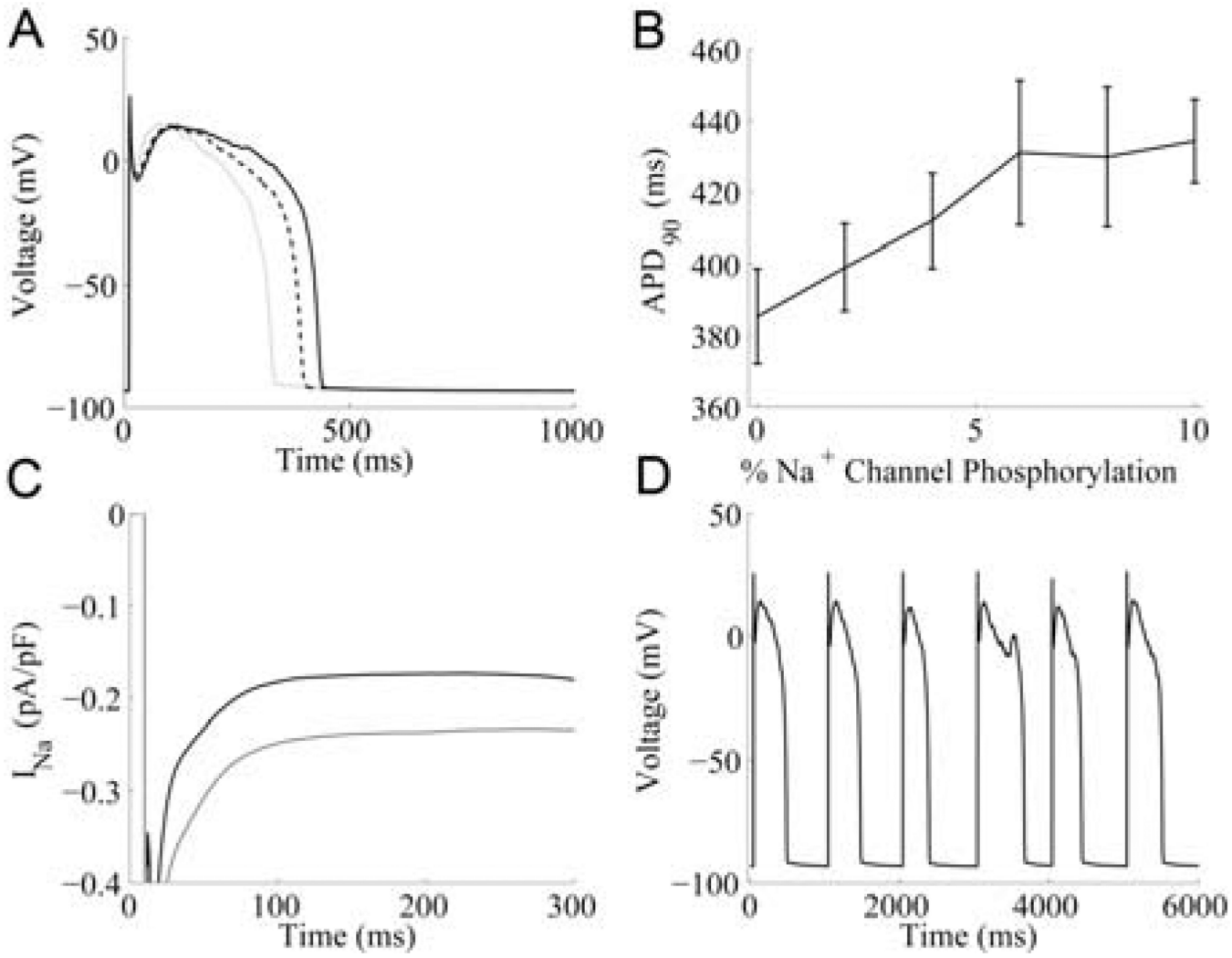

Fig. 3.

Simulated late I_{Na} and APD. (A) Average simulated APs at 0.5 Hz (solid black line), 1 Hz (dotted line), and 2 Hz pacing (solid grey line). (B) APD_{90} as a function of Na^+ channel phosphorylation (mean ± S.E.M.) . (C) Average late I_{Na} underlying steady-state 1-Hz APs with 0% (black) and 10% (grey) Na^+ channel phosphorylation. (D) Simulated EAD at 1-Hz with 10% Na^+ channels phosphorylated.

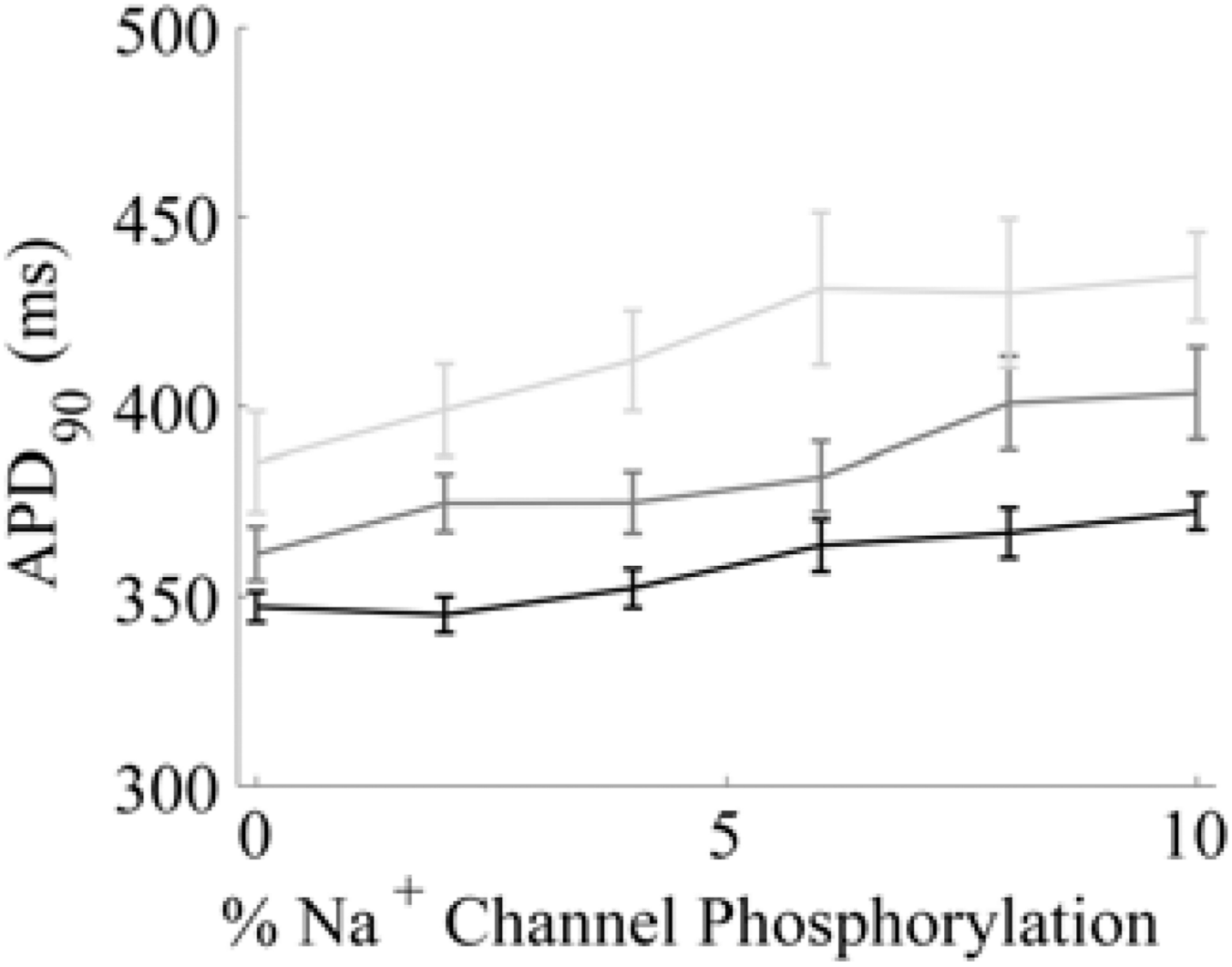

Fig. 4.

APD as a function of LCC and Na^+ channel phosphorylation (1-Hz pacing). Mean APD_{90} ± S.E.M. is shown (n = 30). Black: reduction of LCC phosphorylation rate to 60% of control (~1.4% LCCs phosphorylated); dark grey curve: reduction of LCC phosphorylation rate to 80% of control (~2.5% LCCs phosphorylated); light grey curve: control LCC phosphorylation rate (~3.9% LCCs phosphorylated).

TABLE I

Na^+ Channel Parameters

	Unphosphorylated		Phosphorylated	
Parameter	**23 °C**	**37 °C**	**23 °C**	**37 °C**
P_{1a1}	7.9852	3.9926	7.9852	3.9926
P_{2a1}	0.0204	0.0204	0.0204	0.0204
P_{1a4}	1.1516	5.758	1.1516	5.758
P_{2a4}	26.9168	107.6672	26.9168	107.6672
P_{1a5}	6.5×10^{-9}	1.625×10^{-8}	1.0×10^{-8}	2.5×10^{-8}
P_{2a5}	6.2134	6.2134	6.2134	6.2134
P_{1b1}	0.0012	0.003	0.0012	0.003
P_{2b1}	9.3532	9.3532	9.3532	9.3532
P_{1b2}	0.0147	0.0367	0.0147	0.0367
P_{2b2}	6.6636	6.6636	6.6636	6.6636
P_{1b3}	6.7×10^{-4}	1.675×10^{-3}	6.7×10^{-4}	1.675×10^{-3}
P_{2b3}	17.3338	17.3338	17.3338	17.3338
P_{1b5}	0.0053	0.0132	0.0037	0.0132
P_{2b5}	-2.88×10^{-6}	-7.2×10^{-6}	-1.82×10^{-6}	-4.55×10^{-6}
P_{1a6}	27.2731	27.2731	1.9948	1.9948
P_{1b6}	9.8×10^{-7}	2.45×10^{-6}	1.51×10^{-6}	3.775×10^{-6}
P_{2b6}	11.7989	11.7989	11.7989	11.7989
P_{1a7}	0.0019	0.0047	0.0007	0.0018
P_{2a7}	25.9073	25.9073	151.5985	151.5985
P_{1b7}	0.0012	0.003	0.0012	0.003
P_{2b7}	53.4430	53.4430	53.4430	53.4430
P_{1a8}	6.46×10^{-7}	1.615×10^{-6}	5.17×10^{-6}	7.238×10^{-6}
P_{1b8}	6.16×10^{-4}	1.54×10^{-3}	6.16×10^{-4}	1.54×10^{-3}
P_{1a4_2}	1.2109	1.2109	0.4089	0.1022